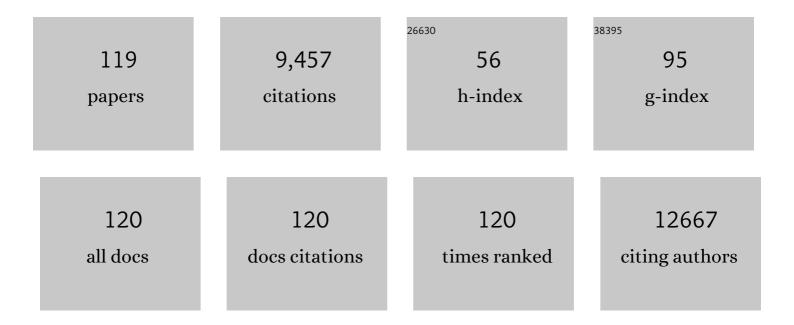


List of Publications by Year in descending order

Source: https://exaly.com/author-pdf/8286435/publications.pdf

Version: 2024-02-01



#	Article	IF	CITATIONS
1	Photocatalysts with internal electric fields. Nanoscale, 2014, 6, 24-42.	5.6	654
2	Recent progress on sodium ion batteries: potential high-performance anodes. Energy and Environmental Science, 2018, 11, 2310-2340.	30.8	561
3	Transition metal based battery-type electrodes in hybrid supercapacitors: A review. Energy Storage Materials, 2020, 28, 122-145.	18.0	413
4	Biomass derived interconnected hierarchical micro-meso-macro- porous carbon with ultrahigh capacitance for supercapacitors. Carbon, 2019, 147, 540-549.	10.3	374
5	Advances in non-enzymatic glucose sensors based on metal oxides. Journal of Materials Chemistry B, 2016, 4, 7333-7349.	5.8	348
6	Porous Two-Dimensional Materials for Photocatalytic and Electrocatalytic Applications. Matter, 2020, 2, 1377-1413.	10.0	254
7	A novel border-rich Prussian blue synthetized by inhibitor control as cathode for sodium ion batteries. Nano Energy, 2017, 39, 273-283.	16.0	208
8	Extreme ultraviolet resist materials for sub-7 nm patterning. Chemical Society Reviews, 2017, 46, 4855-4866.	38.1	185
9	Rapid microwave-assisted synthesis of Mn3O4–graphene nanocomposite and its lithium storage properties. Journal of Materials Chemistry, 2012, 22, 3600.	6.7	183
10	Advanced High Energy Density Secondary Batteries with Multiâ€Electron Reaction Materials. Advanced Science, 2016, 3, 1600051.	11.2	180
11	Bioâ€Nanotechnology in Highâ€Performance Supercapacitors. Advanced Energy Materials, 2017, 7, 1700592.	19.5	168
12	Green Synthesis of Fluorescent Carbon Dots from Gynostemma for Bioimaging and Antioxidant in Zebrafish. ACS Applied Materials & Interfaces, 2019, 11, 9832-9840.	8.0	168
13	Design of surface protective layer of LiF/FeF3 nanoparticles in Li-rich cathode for high-capacity Li-ion batteries. Nano Energy, 2015, 15, 164-176.	16.0	162
14	An Effective Approach To Protect Lithium Anode and Improve Cycle Performance for Li–S Batteries. ACS Applied Materials & Interfaces, 2014, 6, 15542-15549.	8.0	157
15	Double Soft-Template Synthesis of Nitrogen/Sulfur-Codoped Hierarchically Porous Carbon Materials Derived from Protic Ionic Liquid for Supercapacitor. ACS Applied Materials & Interfaces, 2017, 9, 26088-26095.	8.0	142
16	Poly(vinyl alcohol)-Assisted Fabrication of Hollow Carbon Spheres/Reduced Graphene Oxide Nanocomposites for High-Performance Lithium-Ion Battery Anodes. ACS Nano, 2018, 12, 4824-4834.	14.6	141
17	An investigation of functionalized electrolyte using succinonitrile additive for high voltage lithium-ion batteries. Journal of Power Sources, 2016, 306, 70-77.	7.8	140
18	Chemical Inhibition Method to Synthesize Highly Crystalline Prussian Blue Analogs for Sodium-Ion Battery Cathodes. ACS Applied Materials & Interfaces, 2016, 8, 31669-31676.	8.0	139

#	Article	IF	CITATIONS
19	A durable half-metallic diatomic catalyst for efficient oxygen reduction. Energy and Environmental Science, 2022, 15, 1601-1610.	30.8	137
20	Advanced cathode materials for lithium-ion batteries using nanoarchitectonics. Nanoscale Horizons, 2016, 1, 423-444.	8.0	119
21	Surface Modification of Li-Rich Cathode Materials for Lithium-Ion Batteries with a PEDOT:PSS Conducting Polymer. ACS Applied Materials & amp; Interfaces, 2016, 8, 23095-23104.	8.0	119
22	Self-assembly of hierarchical star-like Co3O4 micro/nanostructures and their application in lithium ion batteries. Nanoscale, 2013, 5, 1922.	5.6	117
23	High performance hydrophilic pervaporation composite membranes for water desalination. Desalination, 2014, 347, 199-206.	8.2	109
24	SnSb@carbon nanocable anchored on graphene sheets for sodium ion batteries. Nano Research, 2014, 7, 1466-1476.	10.4	108
25	Hollow Sphere TiO ₂ –ZrO ₂ Prepared by Self-Assembly with Polystyrene Colloidal Template for Both Photocatalytic Degradation and H ₂ Evolution from Water Splitting. ACS Sustainable Chemistry and Engineering, 2016, 4, 2037-2046.	6.7	106
26	Ammonia-induced robust photocatalytic hydrogen evolution of graphitic carbon nitride. Nanoscale, 2015, 7, 18887-18890.	5.6	105
27	Dual templating fabrication of hierarchical porous three-dimensional ZnO/carbon nanocomposites for enhanced photocatalytic and photoelectrochemical activity. Applied Catalysis B: Environmental, 2018, 222, 209-218.	20.2	105
28	Electrostatic Self-Assembly of Sandwich-Like CoAl-LDH/Polypyrrole/Graphene Nanocomposites with Enhanced Capacitive Performance. ACS Applied Materials & Interfaces, 2017, 9, 31699-31709.	8.0	103
29	Synthesis of Mn3O4-anchored graphene sheet nanocomposites via a facile, fast microwave hydrothermal method and their supercapacitive behavior. Electrochimica Acta, 2013, 87, 801-808.	5.2	101
30	Scalable synthesis of self-standing sulfur-doped flexible graphene films as recyclable anode materials for low-cost sodium-ion batteries. Carbon, 2016, 107, 67-73.	10.3	101
31	Trapping sulfur in hierarchically porous, hollow indented carbon spheres: a high-performance cathode for lithium–sulfur batteries. Journal of Materials Chemistry A, 2016, 4, 9526-9535.	10.3	100
32	Synthesis and electrochemical performance of cathode material Li1.2Co0.13Ni0.13Mn0.54O2 from spent lithium-ion batteries. Journal of Power Sources, 2014, 249, 28-34.	7.8	98
33	Facile synthesis of a MoO2–Mo2C–C composite and its application as favorable anode material for lithium-ion batteries. Journal of Power Sources, 2016, 307, 552-560.	7.8	98
34	Synthesis, characterization, and electrochemistry of cathode material Li[Li0.2Co0.13Ni0.13Mn0.54]O2 using organic chelating agents for lithium-ion batteries. Journal of Power Sources, 2013, 228, 206-213.	7.8	97
35	Preparation of Prussian Blue Submicron Particles with a Pore Structure by Two-Step Optimization for Na-Ion Battery Cathodes. ACS Applied Materials & amp; Interfaces, 2016, 8, 16078-16086.	8.0	95
36	Na2NixCo1â^'xFe(CN)6: A class of Prussian blue analogs with transition metal elements as cathode materials for sodium ion batteries. Electrochemistry Communications, 2015, 59, 91-94.	4.7	93

#	Article	IF	CITATIONS
37	Visible light photochemical activity of heterostructured PbTiO3–TiO2 core–shell particles. Catalysis Science and Technology, 2012, 2, 1945.	4.1	90
38	Construction of Z-scheme carbon nanodots/WO ₃ with highly enhanced photocatalytic hydrogen production. Journal of Materials Chemistry A, 2015, 3, 8256-8259.	10.3	85
39	Interconnected honeycomb-like porous carbon derived from plane tree fluff for high performance supercapacitors. Journal of Materials Chemistry A, 2016, 4, 10869-10877.	10.3	83
40	Intramolecular Hydrogen Bonds Quench Photoluminescence and Enhance Photocatalytic Activity of Carbon Nanodots. Chemistry - A European Journal, 2015, 21, 8561-8568.	3.3	75
41	Anisotropic thermal conductivity of graphene wrinkles. Nanoscale, 2014, 6, 5703-5707.	5.6	74
42	Photocatalytic overall water splitting by graphitic carbon nitride. InformaÄnÃ-Materiály, 2021, 3, 931-961.	17.3	74
43	Studying the Mechanism of Hybrid Nanoparticle Photoresists: Effect of Particle Size on Photopatterning. Chemistry of Materials, 2015, 27, 5027-5031.	6.7	73
44	Fabrication of Hierarchical Porous Carbon Nanoflakes for High-Performance Supercapacitors. ACS Applied Materials & Interfaces, 2017, 9, 34944-34953.	8.0	72
45	A novel fabrication strategy for doped hierarchical porous biomass-derived carbon with high microporosity for ultrahigh-capacitance supercapacitors. Journal of Materials Chemistry A, 2019, 7, 19939-19949.	10.3	71
46	Heterostructured Ceramic Powders for Photocatalytic Hydrogen Production: Nanostructured <scp><scp>TiO</scp></scp> ₂ Shells Surrounding Microcrystalline (<scp><scp>Ba</scp></scp> , <scp>Sr</scp>) <scp>TiO</scp> 3 Cores. Journal of the American Ceramic Society, 2012, 95, 1414-1420.	3.8	70
47	Microwave/freeze casting assisted fabrication of carbon frameworks derived from embedded upholder in tremella for superior performance supercapacitors. Energy Storage Materials, 2019, 18, 447-455.	18.0	70
48	Bio-inspired design of hierarchical PDMS microstructures with tunable adhesive superhydrophobicity. Nanoscale, 2015, 7, 6151-6158.	5.6	69
49	Controllable synthesis of RGO/Fe _x O _y nanocomposites as high-performance anode materials for lithium ion batteries. Journal of Materials Chemistry A, 2014, 2, 9844-9850.	10.3	68
50	Surface Hydrophilicity and Structure of Hydrophilic Modified PVDF Membrane by Nonsolvent Induced Phase Separation and Their Effect on Oil/Water Separation Performance. Industrial & Engineering Chemistry Research, 2014, 53, 6401-6408.	3.7	68
51	Synthesis of hollow GeO2 nanostructures, transformation into Ge@C, and lithium storage properties. Journal of Materials Chemistry A, 2013, 1, 7666.	10.3	66
52	Selfâ€Regulative Nanogelator Solid Electrolyte: A New Option to Improve the Safety of Lithium Battery. Advanced Science, 2016, 3, 1500306.	11.2	63
53	Sandwich-like graphene/polypyrrole/layered double hydroxide nanowires for high-performance supercapacitors. Journal of Power Sources, 2016, 331, 67-75.	7.8	62
54	High visible light photocatalytic activities obtained by integrating g-C3N4 with ferroelectric PbTiO3. Journal of Materials Science and Technology, 2021, 74, 128-135.	10.7	62

#	Article	IF	CITATIONS
55	Recent progress of phosphorus composite anodes for sodium/potassium ion batteries. Energy Storage Materials, 2021, 34, 436-460.	18.0	61
56	Hierarchical carbon-coated acanthosphere-like Li4Ti5O12 microspheres for high-power lithium-ion batteries. Journal of Power Sources, 2016, 314, 18-27.	7.8	59
57	Fabrication of Hierarchical Porous Carbon Frameworks from Metal-Ion-Assisted Step-Activation of Biomass for Supercapacitors with Ultrahigh Capacitance. ACS Sustainable Chemistry and Engineering, 2019, 7, 10763-10772.	6.7	56
58	Quantum dot heterostructure with directional charge transfer channels for high sodium storage. Energy Storage Materials, 2021, 39, 278-286.	18.0	56
59	Facile synthesis of graphene–molybdenum dioxide and its lithium storage properties. Journal of Materials Chemistry, 2012, 22, 16072.	6.7	53
60	Surfactant-free self-assembly of reduced graphite oxide-MoO2 nanobelt composites used as electrode for lithium-ion batteries. Electrochimica Acta, 2016, 211, 972-981.	5.2	53
61	Remarkable supercapacitor performance of petal-like LDHs vertically grown on graphene/polypyrrole nanoflakes. Journal of Materials Chemistry A, 2017, 5, 8964-8971.	10.3	53
62	A strongly coupled CoS2/ reduced graphene oxide nanostructure as an anode material for efficient sodium-ion batteries. Journal of Alloys and Compounds, 2017, 726, 394-402.	5.5	53
63	Polyethyleneâ€Glycolâ€Doped Polypyrrole Increases the Rate Performance of the Cathode in Lithium–Sulfur Batteries. ChemSusChem, 2013, 6, 1438-1444.	6.8	52
64	Visible-Light Photochemical Activity of Heterostructured Core–Shell Materials Composed of Selected Ternary Titanates and Ferrites Coated by TiO ₂ . ACS Applied Materials & Interfaces, 2013, 5, 5064-5071.	8.0	51
65	Solubility studies of inorganic–organic hybrid nanoparticle photoresists with different surface functional groups. Nanoscale, 2016, 8, 1338-1343.	5.6	51
66	Combinatorial substrate epitaxy: A high-throughput method for determining phase and orientation relationships and its application to BiFeO3/TiO2 heterostructures. Acta Materialia, 2012, 60, 6486-6493.	7.9	49
67	Synthesis of Co-based Prussian Blue Analogues/Dual-Doped Hollow Carbon Microsphere Hybrids as High-Performance Bifunctional Electrocatalysts for Oxygen Evolution and Overall Water Splitting. ACS Sustainable Chemistry and Engineering, 2020, 8, 8318-8326.	6.7	45
68	Heterostructured (Ba,Sr)TiO3/TiO2 core/shell photocatalysts: Influence of processing and structure on hydrogen production. International Journal of Hydrogen Energy, 2013, 38, 6948-6959.	7.1	43
69	The design of underwater superoleophobic Ni/NiO microstructures with tunable oil adhesion. Nanoscale, 2015, 7, 19293-19299.	5.6	43
70	Influence of tunable pore size on photocatalytic and photoelectrochemical performances of hierarchical porous TiO2/C nanocomposites synthesized via dual-Templating. Applied Catalysis B: Environmental, 2018, 224, 341-349.	20.2	43
71	Rational construction of MoS ₂ /Mo ₂ N/C hierarchical porous tubular nanostructures for enhanced lithium storage. Journal of Materials Chemistry A, 2019, 7, 23886-23894.	10.3	43
72	Dual templated synthesis of tri-modal porous SrTiO3/TiO2@ carbon composites with enhanced photocatalytic activity. Applied Catalysis A: General, 2019, 575, 132-141.	4.3	42

#	Article	IF	CITATIONS
73	Ferroelectric Oxide Nanocomposites with Trimodal Pore Structure for High Photocatalytic Performance. Nano-Micro Letters, 2019, 11, 37.	27.0	39
74	V 2 O 5 /Mesoporous Carbon Composite as a Cathode Material for Lithium-ion Batteries. Electrochimica Acta, 2015, 173, 172-177.	5.2	36
75	Study on the polarity, solubility, and stacking characteristics of asphaltenes. Fuel, 2014, 128, 366-372.	6.4	35
76	Stabilization of NaZn(BH ₄) ₃ via nanoconfinement in SBA-15 towards enhanced hydrogen release. Journal of Materials Chemistry A, 2013, 1, 250-257.	10.3	34
77	Synthesis and Characterization of Cobalt-Doped WS2 Nanorods for Lithium Battery Applications. Nanoscale Research Letters, 2010, 5, 1301-1306.	5.7	33
78	Preparation of octahedral CuO micro/nanocrystals and electrochemical performance as anode for lithium-ion battery. Journal of Alloys and Compounds, 2014, 600, 162-167.	5.5	32
79	Engineering Highâ€Performance MoO ₂ â€Based Nanomaterials with Supercapacity and Superhydrophobicity by Tuning the Raw Materials Source. Small, 2018, 14, e1800480.	10.0	32
80	Functionalization of polyacrylonitrile nanofiber using ATRP method for boric acid removal from aqueous solution. Journal of Water Process Engineering, 2014, 3, 98-104.	5.6	30
81	A hierarchical Zn ₂ Mo ₃ O ₈ nanodots–porous carbon composite as a superior anode for lithium-ion batteries. Chemical Communications, 2016, 52, 9402-9405.	4.1	29
82	Post-wrinkling analysis of a torsionally sheared annular thin film by using a compound series method. International Journal of Mechanical Sciences, 2016, 110, 22-33.	6.7	27
83	The effects of FEC (fluoroethylene carbonate) electrolyte additive on the lithium storage properties of NiO (nickel oxide) nanocuboids. Energy, 2013, 58, 707-713.	8.8	26
84	Construction of 3D porous MXene supercapacitor electrode through a dual-step freezing strategy. Scripta Materialia, 2022, 213, 114605.	5.2	25
85	Characteristic performance of SnO/Sn/Cu6Sn5 three-layer anode for Li-ion battery. Electrochimica Acta, 2013, 109, 46-51.	5.2	24
86	Preparation and characterization of asymmetric polyarylene sulfide sulfone (PASS) solvent-resistant nanofiltration membranes. Materials Letters, 2014, 132, 11-14.	2.6	23
87	Poly(N,N-dimethylaminoethyl methacrylate) modification of a regenerated cellulose membrane using ATRP method for copper(ii) ion removal. RSC Advances, 2013, 3, 20625.	3.6	22
88	Oxide Nanoparticle EUV (ONE) Photoresists: Current Understanding of the Unusual Patterning Mechanism. Journal of Photopolymer Science and Technology = [Fotoporima Konwakai Shi], 2015, 28, 515-518.	0.3	21
89	Overall Photocatalytic Water Splitting of Crystalline Carbon Nitride with Facet Engineering. CheM, 2020, 6, 2439-2441.	11.7	21
90	Boosting sodium storage performance of Mo2C via nitrogen-doped carbon sphere encapsulation and rGO wrapping. Chemical Engineering Journal, 2021, 413, 127471.	12.7	21

#	Article	IF	CITATIONS
91	Molten-salt synthesis of crystalline C3N4/C nanosheet with high sodium storage capability. Chemical Engineering Journal, 2021, 425, 131591.	12.7	20
92	Advantageous Tubular Structure of Biomass-Derived Carbon for High-Performance Sodium Storage. ACS Applied Energy Materials, 2021, 4, 4955-4965.	5.1	18
93	Photocatalytic overall water splitting of carbon nitride by band-structure modulation. Matter, 2021, 4, 1765-1767.	10.0	17
94	Constructing Crystalline gâ€C ₃ N ₄ /gâ€C ₃ N _{4â^'x} S _x lsotype Heterostructure for Efficient Photocatalytic and Piezocatalytic Performances. Energy and Environmental Materials, 2023, 6, .	12.8	17
95	Fabrication of hierarchical gecko-inspired microarrays using a three-dimensional porous nickel oxide template. Journal of Materials Chemistry B, 2015, 3, 6571-6575.	5.8	14
96	Increasing sensitivity of oxide nanoparticle photoresists. , 2014, , .		13
97	A novel fabrication approach for three-dimensional hierarchical porous metal oxide/carbon nanocomposites for enhanced solar photocatalytic performance. Catalysis Science and Technology, 2017, 7, 1965-1970.	4.1	13
98	The influence of polyamic acid molecular weight on the membrane structure and performance of polyimide solventâ€resistant nanofiltration. Journal of Chemical Technology and Biotechnology, 2016, 91, 777-785.	3.2	12
99	Enhanced stability and rate performance of zinc-doped cobalt hexacyanoferrate (CoZnHCF) by the limited crystal growth and reduced distortion. Journal of Energy Chemistry, 2022, 69, 649-658.	12.9	12
100	Influence of Ultrasonication Conditions on the Structure and Performance of Poly(vinylidene) Tj ETQq0 0 0 rgBT Research, 2014, 53, 8228-8234.	/Overlock 3.7	10 Tf 50 387 11
101	Fabrication of Highâ€Performance Biomass Derived Carbon/Metal Oxide Photocatalysts with Trilevel Hierarchical Pores from Organic–Inorganic Network. Advanced Sustainable Systems, 2019, 3, 1800169.	5.3	11
102	Molten salt assisted fabrication of ferroelectric BaTiO3 based cathode for high-performance lithium sulfur batteries. Chemical Engineering Journal, 2022, 435, 135031.	12.7	11
103	Study on the dipole moment of asphaltene molecules through dielectric measuring. Fuel, 2015, 140, 609-615.	6.4	10
104	Facile fabrication of hierarchical micro-meso-macro porous metal oxide with high photochemical and electrochemical performances. Applied Surface Science, 2019, 465, 672-677.	6.1	10
105	Non-aqueous negative-tone development of inorganic metal oxide nanoparticle photoresists for next generation lithography. Proceedings of SPIE, 2013, , .	0.8	7
106	Mode jumping analysis of thin film secondary wrinkling. International Journal of Mechanical Sciences, 2015, 104, 138-146.	6.7	7
107	Crystallinity Modulation of Electron Acceptor in Oneâ€Photon Excitation Pathwayâ€Based Heterostructure for Visibleâ€Light Photocatalysis. Solar Rrl, 2022, 6, 2100901.	5.8	7
108	Influence of Surface Structure on the Capacity and Irreversible Capacity Loss of Sn-Based Anodes for Lithium Ion Batteries. ACS Sustainable Chemistry and Engineering, 2014, 2, 1857-1863.	6.7	6

#	Article	IF	CITATIONS
109	Influence of Morphology and Structure on Electrochemical Performances of Li-Ion Battery Sn Anodes. Metallurgical and Materials Transactions A: Physical Metallurgy and Materials Science, 2018, 49, 5930-5935.	2.2	6
110	Synthesis of pHâ€responsive polyethylene terephthalate trackâ€etched membranes by grafting hydroxyethylâ€methacrylate using atomâ€transfer radical polymerization method. Journal of Applied Polymer Science, 2014, 131, .	2.6	5
111	Abnormal frequency characteristics of wrinkled graphene. RSC Advances, 2014, 4, 9395.	3.6	5
112	Charge transfer resistance of copper and nickel thin film electrodes in nano dimensions. Materials Letters, 2017, 198, 61-64.	2.6	5
113	Electrochemical performances of Cu6Sn5-modified Sn anode with multi-layer structure for Li-ion cell. RSC Advances, 2013, 3, 18339.	3.6	4
114	Investigation on the Oxidation and Reduction of Titanium in Molten Salt with the Soluble TiC Anode. Metallurgical and Materials Transactions E, 2015, 2, 250-254.	0.5	4
115	Charge transfer resistance of IB and VIB family electrodes in 1 M Na2SO4. Materials Letters, 2017, 207, 187-189.	2.6	4
116	New developments in ligand-stabilized metal oxide nanoparticle photoresists for EUV lithography. Proceedings of SPIE, 2015, , .	0.8	3
117	Fabrication of Metal-Doped Hierarchical Trimodal Porous Li3V2(PO4)3/C Composites with Enhanced Electrochemical Performances for Lithium-Ion Batteries. Metallurgical and Materials Transactions A: Physical Metallurgy and Materials Science, 2019, 50, 1468-1479.	2.2	3
118	Relationships between Electrical Conductivity Variation and Coking Characteristics of Residue during Thermal Reaction through Online Equipment. Energy & Fuels, 2016, 30, 5404-5410.	5.1	2
119	Studying the mechanism of hybrid nanoparticle EUV photoresists. Proceedings of SPIE, 2015, , .	0.8	0